Food Control 162 (2024) 110441

Contents lists available at ScienceDirect

Food Control

journal homepage: www.elsevier.com/locate/foodcont

Enhancement of riboflavin-mediated photodynamic inactivation against *Salmonella* on tuna fillets coupled with slightly basic electrolyzed water

Jing Jing Wang [a,b,d,e], Tiantian He [a,d,e], Huihui Li [b], Hao Dong [c], Yang Liu [a,d,e], Qiaohui Zeng [a,*], Yong Zhao [b,**]

[a] Guangdong Provincial Key Laboratory of Intelligent Food Manufacturing, Foshan University, Foshan, 528225, China
[b] College of Food Science and Technology, Shanghai Ocean University, Shanghai, 201306, China
[c] Zhongkai University of Agriculture and Engineering, College of Light Industry and Food Sciences, Guangzhou, 510225, China
[d] National Technical Center (Foshan) for Quality Control of Famous and Special Agricultural Products, Foshan, 528225, China
[e] Foshan Research Center for Quality Safety of the Whole Industry Chain of Agricultural Products, Foshan, 528225, China

ARTICLE INFO

Keywords:
Photodynamic inactivation
Slightly basic electrolyzed water
Reactive oxygen species (ROS)
Salmonella
Riboflavin
Pathogens

ABSTRACT

This study aimed to develop an efficient PDI system to kill *Salmonella* in solution or on tuna fillets under 455 nm blue light-emitting diodes (LED) irradiation, by selecting slightly basic electrolyzed water (SBEW) as the solvent. Results showed that the solvent of SBEW increased the solubility of riboflavin, and notably strengthened the production of ROS compared to normal saline solution. On this basis, the riboflavin-mediated PDI coupled with SBEW enhanced the inactivation of *Salmonella*, supported by that the viability of *Salmonella* was significantly ($P < 0.05$) inactivated by 5.02 Log_{10} CFU/mL with 9.36 J/cm^2 irradiation and 80 μM riboflavin, and no viable cells were detected when the irradiation dose was increased to 12.48 J/cm^2. The action mechanisms showed that this novel PDI damaged the cell membrane causing the leakage of cellular contents, degraded the genomic DNA and enhanced the lipid peroxidation in *Salmonella*. In addition, the PDI system efficiently killed >4.0 Log_{10} CFU/g of *Salmonella* on tuna fillets with 120 μM riboflavin and 18.72 J/cm^2 irradiation. Furthermore, the PDI system decelerated the proliferation of *Salmonella*, the changes of electrical conductivity, pH and color, and lipid oxidation in tuna fillets during the storage. This study provides a promising PDI system to control food pathogen contamination and preserve the storage quality of seafood.

1. Introduction

Salmonella is a bacterial pathogen that easily contaminates foods to threaten the public health (Yue et al., 2020). In China, *Salmonella* is also one of the most important foodborne pathogens, and it is estimated that about 70–80% of foodborne disease outbreaks are caused by the ingestion of livestock and poultry products infected with *Salmonella* (Wang et al., 2007; Zhang et al., 2018). To control this pathogen, traditional heating and chemical disinfectants are often used, but developing novel non-thermal antibacterial technologies are pressing by considering their unacceptable effects on food quality and safety (Liu et al., 2017; Luksiene et al., 2009).

Photodynamic Inactivation (PDI) is a non-thermal antibacterial technology, and it consists of three indispensable elements: light, photosensitizer, and oxygen (Dolmans et al., 2003). This combination leads to the production of reactive oxygen species (ROS), including hydrogen peroxide (H_2O_2), singlet oxygen ($^1O_2$), superoxide anion ($O_2^{\bullet-}$), and hydroxyl radical (•OH) etc., which can oxidize the biological macromolecules to disable cells (Alves et al., 2015). The photosensitizer is a key factor in influencing the potency of PDI, because it directly absorbs light energy and transfers it to O_2 molecules by a serial of reactions, and finally generates ROS (Hong et al., 2016). Generally, the maximum absorption spectrum of photosensitizer should have a clear spectral overlap with the maximum emission spectrum of light (Chen et al., 2020), which can promote the success of PDI system.

Various photosensitizers have been applied to construct PDI system (Sadraeian et al., 2022). Thereinto, the natural food-grade photosensitizers (e.g., riboflavin, curcumin) are allowed in the food industry owing to the food safety issues. Our group previously demonstrated that the riboflavin-mediated PDI showed difficulties in inactivating *Salmonella*,

* Corresponding author.
** Corresponding author.
E-mail addresses: z_qh2011@163.com (Q. Zeng), yzhao@shou.edu.cn (Y. Zhao).

https://doi.org/10.1016/j.foodcont.2024.110441
Received 14 November 2023; Received in revised form 1 March 2024; Accepted 11 March 2024
Available online 12 March 2024

especially with a low concentration of riboflavin. Only when the concentration of riboflavin reached >150 μM (Li et al., 2021), the riboflavin-mediated PDI could kill ~6.0 Log_{10} CFU/mL planktonic *Salmonella* with 9.36 J/cm^2 of blue LED irradiation, but just reduced 2.1 Log_{10} CFU/g of *Salmonella* on tuna fillets with 93.6 J/cm^2 of irradiation. In addition, riboflavin (RF) is slightly soluble in water and is also easily oxidized to lose its PDI effects, which limits its application in the PDI system (Beztsinna et al., 2016; Ashoori & Saedisomeolia, 2014).

Slightly basic electrolyzed water (SBEW) is a safe and edible water, and notably the SBEW with its alkaline pH ≤ 9.8 can exert biological effects in human body (LeBaron et al., 2022; Rubik, 2011). Notably, the SBEW has a high negative redox potential (−150 mV to −300 mV), a low level of dissolved oxygen and a high permeability (Shirahata et al., 1997), which is highly beneficial for the structural stability and solubility of natural molecules (Henry & Chambron, 2013). On this basis, the SBEW is selected as the solvent to dissolve photosensitizer, which can theoretically induce higher PDI potency in comparison with ordinary water.

Considering all the above facts, the SBEW was innovatively selected as the solvent to dissolve the photosensitizer of riboflavin. Meanwhile, the inactivation potency of this novel PDI against *Salmonella* was explored, and its action mechanism was elucidated by monitoring the changes of ROS production, DNA integrity, proteins, cell membrane, alkaline phosphatase (ALP) activity, and lipid peroxide (LPO). Furthermore, the bactericidal efficiency of PDI against *Salmonella* on the tuna fillets was investigated, and the effects of the novel PDI system on preserving the storage quality of tuna fillets were also explored. This study will facilitate the development of novel PDI to guarantee food safety in the future.

2. Materials and methods

2.1. Bacterial strains culture and preparation

A cocktail of *Salmonella* Typhimurium CICC21484 and Salmonella Enteritidis CMCC 50041 was used. Salmonella Typhimurium CICC21484 was bought from China Center of Industrial Culture Collection (CICC) and *Salmonella* Enteritidis CMCC 50041 was bought from China Medical Culture Collection Center (CMCC). All strains were stored in a −80 °C freezer before use, and then were streaked on a bismuth sulfite agar (BSA) plate and incubated at 37 °C for 48 h. A single colony was enriched in 9 mL tryptic soy broth (TSB) at 37 °C for overnight. The pellets were washed two times with 0.85% NaCl after centrifugation and then serially diluted to the initial population ~7 Log_{10} CFU/mL.

2.2. Light-emitting diodes (LED) system, photosensitizer, slightly basic electrolyzed water, experimental procedures of PDI and SBEW treatments

Blue LEDs (455 ± 5 nm, 10 W) were bought from Shenzhen in China (Shenzhen kerun Optoelectronics Inc., China) and selected as the light source. The distance between the LED and bacterial suspension was 5.0 cm and the power density was 5.2 mW/cm^2. The energy dosage was calculated as follows (Chen et al., 2020):

$$E = Pt$$

where E = the energy density, J/cm^2; P = the power density, W/cm^2 and t = time, s.

The riboflavin (RF, food-grade, purity >99.8%, Biotechnology Co., Ltd., Shanghai, China) was selected as the photosensitizer. SBEW was generated using a slightly alkaline electrolyzed water generator (TK-HS90, Panasonic, Japan) and the tap water was directly electrolyzed. The pH and oxidation-reduction potential (ORP) of SBEW was measured as 9.64 ± 0.2 and −388 ± 0.4 mV.

The bacterial suspension was separately mixed with riboflavin to obtain the final riboflavin concentration of 0, 10, 20, 40, 60, 80 and 100 μM. The mixture was incubated for 20 min in dark condition. Subsequently, 500 μL of bacterial suspension was transferred into a 24-well plate, and then exposed to blue LED for 30 min (9.36 J/cm^2). Subsequently, the viable cells were quantified after 10-fold serial dilutions. After incubation at 37 °C for overnight, the colonies of *Salmonella* were counted. For the SBEW groups, the 0.85% NaCl solution was replaced with the solvent of SBEW.

The samples treated without light, riboflavin and SBEW were selected as the negative control (R-L-S-); the samples treated with light but without SBEW were selected as the irradiation control (R-L + S-); the samples only treated with SBEW were selected as the SBEW control (R-L-S+); the samples treated with riboflavin and SBEW were selected as the riboflavin control (R + L-S+); the samples treated with riboflavin and light but without SBEW were selected as the photodynamic control (R + L + S-).

2.3. Visible spectrophotometry analysis

The optical properties of riboflavin in the SBEW were analyzed using a visible spectrophotometer (PERSEE TU-1810, Beijing, China). Briefly, the riboflavin was separately dissolved in 0.85% NaCl solution and SBEW to prepare different concentrations (0–160 μM). Subsequently, the solubility and stability of riboflavin were evaluated by monitoring the spectral changes in the range of 400~750 nm.

2.4. ^{17}O NMR spectra

The ^{17}O NMR full width at half maximum intensity (FWHM) was employed to assess the variations in water cluster size, and generally higher FWHM values generally corresponded to larger water cluster size. ^{17}O NMR experiments were conducted on a Bruker AM 600 superconductor spectrometer, and the sealed capillary tube of D_2O, a locking substance, was inserted at the center of a 5 mm sample tube containing the SBEW or 0.85% NaCl solution. The chemical shifts of the spectra were referenced to the ^{17}O resonance peak of the external D_2O (Li et al., 2006; Yan et al., 2013).

2.5. Reactive oxygen species (ROS) and singlet oxygen ($^1O_2$) detection

ROS was detected by 2,7-dichlorofluorescin diacetate (DCFH-DA, Solarbio Life Sciences, Beijing, China). The fluorescence signal ($\lambda_{ex}/\lambda_{em}$ = 484/525 nm) was determined with a fluorescence spectrophotometer (Hitachi F-4600, Japan) to evaluate intracellular ROS production (Park & Ha, 2020).

Singlet oxygen ($^1O_2$) was determined using 9,10-Anthracenediyl-bis (methylene) dimalonic acid (ADMA) (Sigma Aldrich, America) (Wu et al., 2016). ADMA was mixed with riboflavin to a final concentration 200 μM, and then the mixture was irradiated by blue LED. The decrease of $OD_{400\ nm}$ was expressed as the production of $^1O_2$. The absorbance value of individual ADMA solution or riboflavin solution was recorded as control.

2.5.1. Scanning electron microscopy (SEM)

SEM was performed according to the method of Tan et al. (2021). Briefly, the bacterial suspension was centrifuged, and the pellets were fixed overnight with 0.5 mL of 2.5% glutaraldehyde, and then washed three times with phosphate buffered saline (PBS). The samples were dehydrated with serial ethanol solutions (30%, 50%, 70%, 90% and 100%), and they were coated with gold before SEM observation (SNE-4500 M, JEOL, Japan).

2.6. Analysis of the cell wall integrity

The intracellular alkaline phosphatase (ALP) activity was monitored to analyze the cell wall integrity (Gao et al., 2014). The supernatant of

the treated cells was collected by centrifugation at 6000 rpm for 10 min, and the ALP activity was measured using an alkaline phosphatase assay kit (Jiancheng Reagent Co., Ltd., Nanjing, China). Meanwhile, the supernatant was filtered through a 0.22 μm membrane, and the leakage of intracellular proteins was measured using the BCA assay kit (Solarbio Life Sciences, Beijing, China).

2.7. Lipid oxidation

Lipid oxidation in *Salmonella* was determined by a lipid peroxide (LPO) detection kit (Nanjing Jiancheng Biotechnology Co., LTD.), and the operation was carried out according to the instructions. After PDI treatment, 200 μL of bacterial suspension was used to measure LPO content at 586 nm.

2.8. Sodium dodecyl sulfate polyacrylamide gel electrophoresis (SDS-PAGE) and agarose gel electrophoresis

The treated cells were collected and sonicated for 2 min. After centrifugation, 20 μL of supernatant was mixed with 5 μL loading buffer and heated at 100 °C for 10 min. SDS-PAGE was performed using 12% separation gel and 3% stacking gel. Gels were stained with Coomassie Brilliant Blue (R-250) and destained in methanol-water solution containing 10% acetic acid (0.25% R-250,10% acetic acid, and 45% methanol) (Wang et al., 2017).

The DNA damage was determined by the method of Hu et al. (2018). Briefly, the treated cells were centrifuged at 12,000×*g* for 2 min and the bacterial DNA was extracted using a DNA extraction kit (Tianjin Biotechnology Co., Ltd., Tianjin, China). The product was separated by 2% agarose gel electrophoresis, stained with ethidium bromide, and photographed using the Bio-Rad ChemiDoc™ MP Imaging System.

2.9. Photodynamic treatment of tuna fillets contaminated with Salmonella

The frozen tuna fillets were purchased from a local supermarket in Shanghai, China, and stored at −40 °C before processing. The riboflavin was firstly dissolved in SBEW to reach the final concentrations of 40, 60, 80, 100, 120 μM, and then each tuna sample was inoculated with 100 μL of *Salmonella* (~5.2 Log_{10} CFU/g) by gently spreading. Subsequently, the riboflavin solution was also gently spread onto the surface of tuna fillets, and then incubated for 20 min to guarantee sufficient attachment (Yan et al., 2021; Yu et al., 2021). Afterwards, the samples were exposed to the PDI treatment for 9.36 (30 min), 12.48 (40 min), 18.72 (60 min), 24.90 (80 min) and 31.20 J/cm^2 (100 min). The treated tuna fillets were homogenized in 0.85% NaCl for 2 min, and the supernatant (100 μL) was spread onto Bismuth Sulfite Agar medium to determine the viable cells.

2.10. Low-field nuclear magnetic resonance (LF-NMR) and magnetic resonance imaging (MRI)

The water distribution in tuna fillets was analyzed by LF-NMR (MesoMR23-060 H - I, Niumag Corporation). To prevent water evaporation, the treated tuna fillets (3 cm × 3 cm × 0.5 cm, ~5 g) were covered with polyethylene film. MRI data were obtained using the 0.5 T permanent magnet MiniMR-Rat (Zhang et al., 2016). The pseudo-color picture of proton density was given by using the proton intensity of MATLAB software at different gray values.

2.11. Physical and chemical analysis

The treated tuna fillets were added to 0.85% NaCl and then homogenized for 2 min. The electrical conductivity was measured by an electrical conductivity meter (Metter-Toledo, Zurich, Switzerland). The pH was measured using a pH meter with a polymer pH electrode (Metter-Toledo, Zurich, Switzerland).

Malondialdehyde (MDA) was determined by an MDA assay kit (Solarbio Life Sciences, Beijing, China). The absorbance values of samples were recorded at 523 nm and 600 nm. The amount of MDA was calculated by the following formula: MDA (nmol/g) = 53.763 × (OD_{523nm}-OD_{600nm})/W, where W represents the weight of samples.

2.12. Color analysis

The color changes of tuna fillets were analyzed by Chromatic metre SR-62 (Threenh Technology Co., Ltd., China). The color difference (ΔE) was calculated using the following formula: $\Delta E = [(L^*-L_0)^2+(a^*-a_0)^2+(b^*-b_0)^2]^{1/2}$, and L_0, a_0, and b_0 represent the values of tuna fillets on Day 0.

2.13. Statistical analysis

All data were presented as mean ± standard deviation. Statistical analysis was performed using SPSS 17.0 (SPSS Inc., Chicago, IL). Comparisons between different groups were analyzed through one-way analysis of variance (ANOVA) by unpaired Students' t-test, where the levels of differences were defined at $p < 0.05$.

3. Results and discussion

3.1. Bactericidal potency of PDI coupled with SBEW against Salmonella

The basic physicochemical parameters (including hardness, sulfate and chloride content) of SBEW and tap water were shown in Table S1, and generally, the SBEW presented a lower hardness (88 mg/L), sulfate content (23.9 mg/L) and chloride content (14.1 mg/L) than tap water (102 mg/L hardness, 32.7 mg/L sulfate and 20.1 mg/L chloride). Afterwards, the effects of riboflavin concentration on the inactivation of PDI coupled with SBEW against *Salmonella* are shown in Fig. 1A. In the negative control (R-L-S-), the number of bacterial cells were 6.02 Log_{10} CFU/mL, and no significant ($P > 0.05$) decrease in the colonies were observed in the irradiation control (9.36 J/cm^2, R-L + S-), while a reduction ($P < 0.05$) of ~0.5 Log_{10} CFU/mL of *Salmonella* was found in the SBEW control (R-L-S+), photodynamic control (R + L + S-) and riboflavin control (R + L-S+). Such results were generally consistent with our previous study (Li et al., 2021), reporting that when the irradiation was 9.36 J/cm^2 and the concentration of riboflavin was 100 μM, the riboflavin-mediated PDI only killed ~0.96 Log_{10} CFU/mL of *Salmonella* in 0.85% NaCl solution. With the increase of riboflavin concentration, the PDI coupled with SBEW treatment presented an enhanced ability to kill the cells, and the maximum reduction of populations reached 5.02 Log_{10} CFU/mL with 9.36 J/cm^2 irradiation and 80 μM riboflavin. However, Li et al. (2021) proved that such equivalent reduction was obtained under the action of 150 μM riboflavin and 9.36 J/cm^2 irradiation for the PDI treatment when 0.85% NaCl solution was selected as the solvent to dissolve riboflavin. These results suggest that selecting SBEW as the solvent greatly reduces ~47% usage amount of riboflavin (from 150 μM to 80 μM), and also potentiates the inactivation potency of the riboflavin-mediated PDI against *Salmonella*.

In Fig. 1B, the effects of incubation time on the inactivation of PDI coupled with SBEW against *Salmonella* were investigated. When the incubation time was prolonged to 10 min, the PDI coupled with SBEW treatment reduced ~2.3 Log_{10} CFU/mL of the *Salmonella* cells compared to those samples without the incubation (0 min). With the increase of incubation time to 20 min, the PDI coupled with SBEW treatment greatly ($P < 0.05$) killed the cells by ~5.0 Log_{10} CFU/mL compared to the negative control (6.3 Log_{10} CFU/mL), but the further extension of incubation did not cause a distinct reduction of viable cells ($P > 0.05$). Previous study showed that the common PDI just inactivated 2.5 Log_{10} CFU/mL by selecting the 0.85% NaCl solution as the solvent to dissolve riboflavin (150 μM), under the action of 9.36 J/cm^2 irradiation and 20 min incubation (Li et al., 2021). Based on the results, the

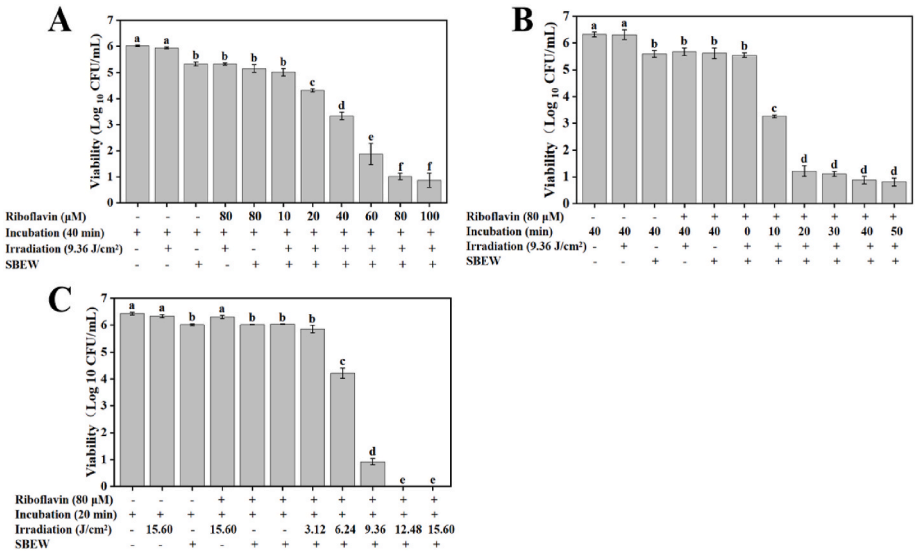

Fig. 1. Effects of the riboflavin-mediated PDI coupled with slightly basic electrolyzed water (SBEW) on the viability of *Salmonella*. (A) Riboflavin concentration; (B) Incubation time; (C) Irradiation time.

riboflavin-mediated PDI coupled with SBEW significantly increased the inactivation of 2.5 Log_{10} CFU/mL of *Salmonella*. (Henry & Chambron, 2013; Tan et al., 2022). On this basis, all these results suggest that the incubation time of 20 min is enough to achieve the adequate interactions between the cells and photosensitizer, thereby effectively inactivating *Salmonella* under the action of PDI.

The irradiation dose of light is a key factor in determining the success of PDI. In Fig. 1C, all control samples did not present an obvious reduction in *Salmonella*. However, the PDI coupled with SBEW decreased ~1.8 Log_{10} CFU/mL of the cells with the increase of the irradiation dose from 3.12 to 6.24 J/cm^2. When the irradiation was increased to 9.36 J/cm^2, a reduction of 5.2 Log_{10} CFU/mL cells was observed, and only <1.0 Log_{10} CFU/mL of the cells were detected in the plates. After the irradiation dose was further increased to 12.48 and 15.60 J/cm^2, no viable cells were detected by the plating method. Considering the irradiation time and bactericidal efficiency of this novel PDI system, the incubation time of 20 min and riboflavin concentration of 80 μM were selected to perform the subsequent investigation about the inactivation mechanism of this PDI against *Salmonella*.

3.2. Action mechanism of PDI coupled with SBEW against Salmonella

Based on the above results and related references (Henry & Chambron, 2013; Tan et al., 2022; Li et al., 2021), the effects of physicochemical properties of SBEW on the structural stability and ROS production of riboflavin were selected as the key research object. In Fig. 2, the visible spectrophotometry was used to explore the structural stability of riboflavin dissolved in SBEW with a light irradiation of 9.36 J/cm^2. The absorption spectra of riboflavin in SBEW or 0.85% NaCl were separately determined. With the increase of riboflavin from 0 to 160 μM, one characteristic peak of riboflavin appeared at 445 nm, and an obvious shift of the peak position was not observed regardless of SBEW or 0.85% NaCl, suggesting that the solvent of SBEW did not cause an obvious damage to the molecular structure of riboflavin. Furthermore, it was found that the peak intensity of riboflavin in the solvent of SBEW was significantly higher than that in 0.85% NaCl solution, indicating that the SBEW exhibited a favorable performance to dissolve riboflavin. Such fact was mainly attributed to the slightly alkaline property of SBEW, because the riboflavin is easily dissolved in alkaline solution (Beztsinna et al., 2016; Ashoori & Saedisomeolia, 2014). In addition, this study also found that the SBEW with a pH of 9.6 presented a relatively higher solubility of riboflavin compared to the 0.85% NaCl solution (pH = 9.6) and the distilled water (pH = 9.6) (Fig. S1). For this point, this study experimentally determined the water cluster size of these two types of solutions, and the results showed that the ^{17}O NMR FWHM of SBEW was 66.49 Hz, and the ^{17}O NMR FWHM of 0.85% NaCl solution was 103.83 Hz (Fig. 3). All these results suggested that the water cluster size of SBEW had a relatively smaller size than that of 0.85% NaCl solution (Li et al., 2006), which further endowed SBEW with an excellent dissolving capacity (Henry & Chambron, 2013; Rubik, 2011). Furthermore, the riboflavin dissolved in SBEW with its concentration of 160 μM had a lower surface tension than that dissolved in 0.85% NaCl solution

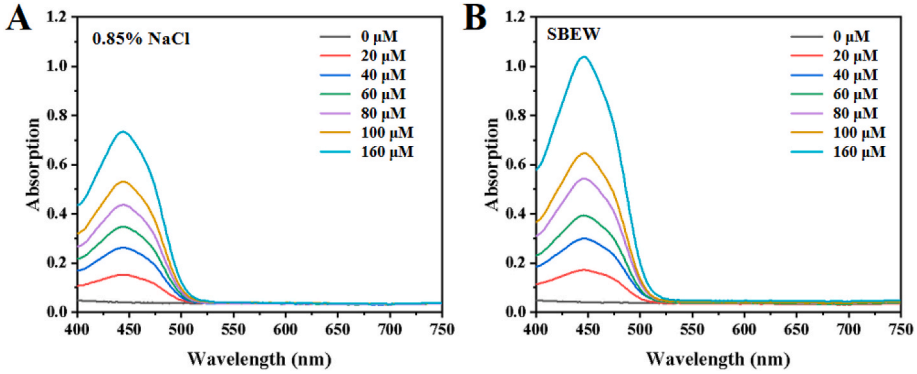

Fig. 2. Absorption spectra of riboflavin with different concentrations in 0.85% NaCl (A) and slightly basic electrolyzed water (SBEW) (B).

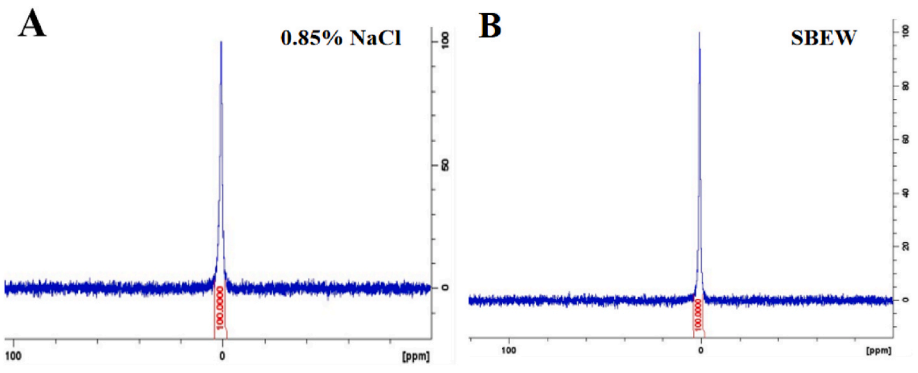

Water sample	^{17}O NMR full width at half maximum intensity (FWHM)
0.85% NaCl	103.83 Hz
Slightly basic electrolyzed water	66.49 Hz

Fig. 3. ^{17}O NMR spectra (A–B) and their full width at half maximum intensity (FWHM) (C) of SBEW and 0.85% NaCl (pH = 9.6).

(Fig. S2), which facilitated the diffusion capacity and wettability of the dissolved photosensitizer to strengthen its adsorption onto the surface of bacterial cells.

The production of ROS is the key element to kill bacterial cells during the PDI process, and generally the higher the level of ROS, the stronger the inactivation potency of PDI (Zhao & Drlica, 2014). The probe of DCFH-DA can be hydrolyzed by cytosolic esterase to DCFH, and then the DCFH is further oxidized to DCF by ROS, and the fluorescence intensity of DCF is analyzed to evaluate the production level of ROS (Rastogi et al., 2010). In Fig. 4A, the riboflavin in 0.85% NaCl solution and SBEW did not present a significant change in the fluorescence intensity of DCF without the light irradiation. When the light irradiation was 9.36 J/cm^2, an obvious increase ($P < 0.05$) in the fluorescence intensity was observed for riboflavin dissolved in the SBEW or 0.85% NaCl solution. However, the riboflavin molecules in the SBEW displayed much higher ($P < 0.05$) fluorescence intensity of DCF than those in 0.85% NaCl solution, indicating that the solvent of SBEW was conducive to the generation of ROS from the riboflavin during the light irradiation.

For all species of ROS, the singlet oxygen ($^1O_2$) is one of the most destructive substances, and it can seriously damage DNA, protein, and other biomacromolecules by penetrating the cell membrane (Wu et al., 2016). On this basis, the production of singlet oxygen ($^1O_2$) was also determined using the ADMA fluorescent probe (Misba et al., 2018), because the reaction between $^1O_2$ and ADMA can reduce the absorption value at 400 nm ($OD_{400\ nm}$). In Fig. 4B, the individual riboflavin (RF) or ADMA did not exhibit evident changes of absorption value ($OD_{400\ nm}$) when they were separately dissolved in the SBEW or 0.85% NaCl. For the riboflavin dissolved in 0.85% NaCl, the absorption value of ADMA showed a gradual decrease with the increase of light irradiation to 9.36 J/cm^2. Notably, the riboflavin dissolved in the SBEW presented a sharp decrease in the absorption value ($OD_{400\ nm}$) of ADMA, and more $^1O_2$ molecules were produced under the same irradiation dose. Overall speaking, all the above-mentioned facts firmly supported that although the dissolved O_2 (8.00 ± 0.21 mg/L) in SBEW is relatively lower than that (6.60 ± 0.07 mg/L) in tap water, the O_2 in SBEW still can be effectively used to generate ROS supported by the results of Fig. 4. More importantly, the SBEW had a relatively smaller water cluster size, which greatly improved the solubility of riboflavin (Figs. 2 and 3). Next, the increased riboflavin molecules absorbed light energy to generate massive ROS (Fig. 4). Moreover, the solution of SBEW and riboflavin had a lower surface tension compared to tap water (Fig. S2), which enhanced the diffusion capacity and wettability of the dissolved photosensitizer onto bacterial cells. Therefore, the generated massive ROS from the adsorbed photosensitizer directly attacked the bacterial cells to achieve an enhanced inactivation effect of PDI.

The inactivation mechanism and targets of PDI coupled with SBEW against *Salmonella* were investigated by monitoring the changes in cell morphology, cell wall integrity, genomic DNA, proteins and lipid peroxidation (LPO). SEM was used to observe the changes in the cell morphology of *Salmonella*. In Fig. 5, all control samples (a_1-a_2, b_1-b_2, c_1-c_2), including R-L-S-, R-L-S+ and R + L + S-, presented a rod-shaped and plump morphology, and no significant changes were observed. By selecting the SBEW as the solvent, the PDI treatment caused a slight deformation and groove on the surface of cells with 3.12 J/cm^2

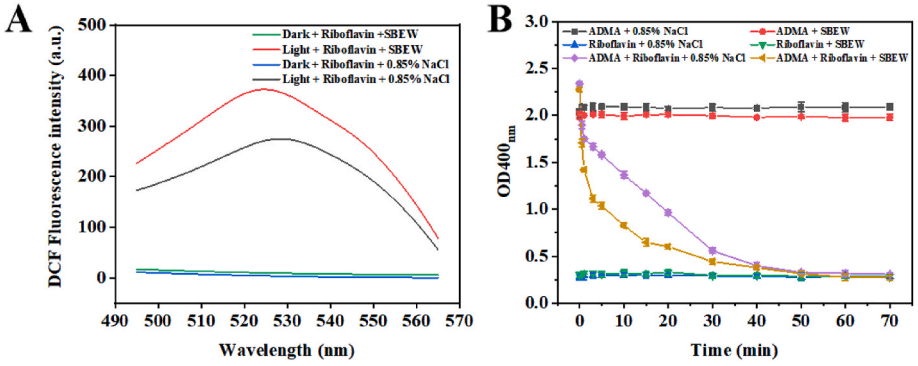

Fig. 4. Effects of slightly basic electrolyzed water (SBEW) on the generation of reactive oxygen species (A) and singlet oxygen (B).

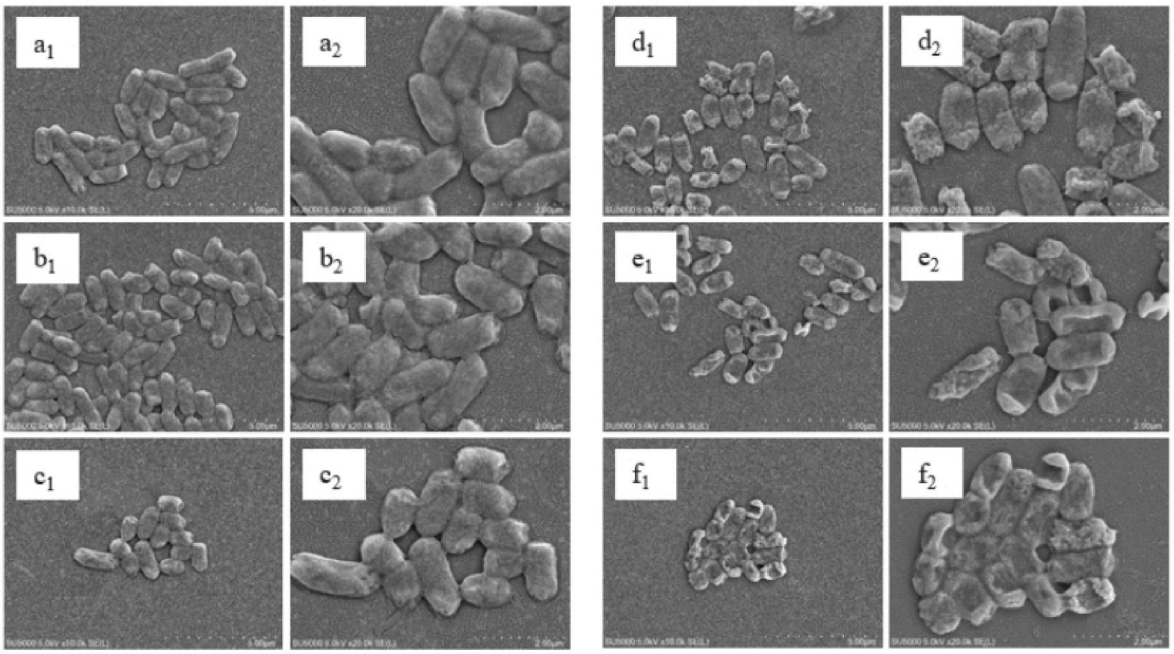

Fig. 5. Effects of the riboflavin-mediated PDI coupled with slightly basic electrolyzed water (SBEW) on the cell morphology of *Salmonella*. (a_1-a_2): R-L-S-; (b_1-b_2): R-L-S+; (c_1-c_2): R + L + S-; (d_1-d_2): R + L + S+: 3.12 J/cm^2 irradiation with 80 μM riboflavin; (e_1-e_2): R + L + S+: 9.36 J/cm^2 irradiation with 80 μM riboflavin; (f_1-f_2): R + L + S+: 15.6 J/cm^2 irradiation with 80 μM riboflavin.

irradiation and 80 μM riboflavin (Fig. 5d_1-d_2). When the irradiation dose was increased to 9.36 J/cm^2, the deformed and shrunk cells of *Salmonella* were clearly observed, and complete collapsed and broken cells appeared with the irradiation dose of 15.6 J/cm^2 (Fig. 5f_1-f_2).

SDS-PAGE was used to evaluate the cellular protein degradation of *Salmonella* treated by the riboflavin-mediated PDI coupled with SBEW. In Fig. 6A, all control samples almost displayed the same bands of proteins (Lane 1, 2, 3 and 4). With the increase of irradiation dose from 3.12 to 15.6 J/cm^2, the riboflavin-mediated PDI coupled with SBEW gradually decreased the band intensities of proteins. Likewise, this novel PDI also destroyed the integrity of DNA, and especially the brightness of DNA bands could hardly be observed when the irradiation dose was

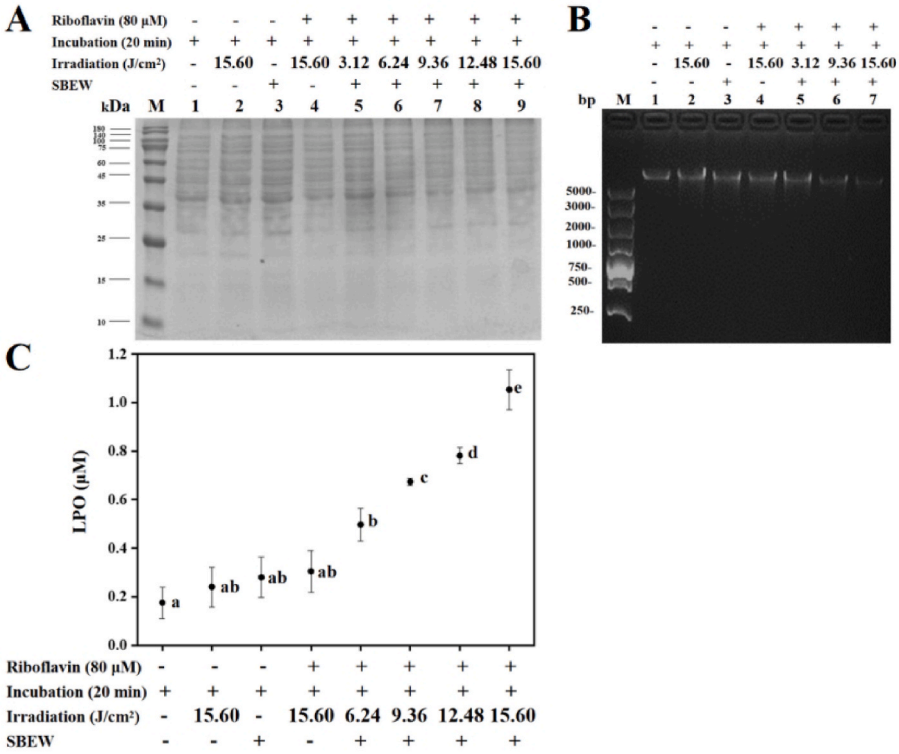

Fig. 6. Effects of the riboflavin-mediated PDI coupled with slightly basic electrolyzed water (SBEW) on the total proteins (A), DNA (B) and lipid peroxide (C) of *Salmonella*.

increased to 9.36 and 15.6 J/cm^2 (Fig. 6B). Considering the above results, it was concluded that the cell wall and genomic DNA in *Salmonella* were vulnerable to be attacked than the cellular proteins by the riboflavin-mediated PDI coupled with SBEW.

Huang et al. (2020) and Chen et al. (2020) found that the curcumin-mediated PDI could easily attack the cytoplasmic DNA of the Gram-positive *Listeria monocytogenes*, but it was difficult to damage the cytoplasmic DNA of the Gram-negative *Vibrio parahaemolyticus*. Our previous study found that the common PDI without SBEW could greatly destroy the cell wall, but barely degraded the genomic DNA of the Gram-negative *Salmonella* with the light irradiation of 9.36 J/cm^2 and 150 μM riboflavin (Li et al., 2021). However, the present study clearly showed that the PDI coupled with SBEW not only destroyed the cell wall, but also degraded the genomic DNA of *Salmonella* with the light irradiation of 9.36 J/cm^2 and 80 μM riboflavin (Figs. 5 and 6). Previous studies showed that the inactivation potency of PDI was jointly influenced by the bacterial species, cellular structure, adsorption capability of photosensitizer onto cells, accessibility of photosensitizer into cells, overlap of emission spectrum and absorption spectrum, etc. (Chen et al., 2020; 2023; Huang et al., 2020). The good dissolving and permeating capacity of SBEW increased the solubility of riboflavin, which finally contributed to the degradation of DNA and proteins under the action of PDI, according to the results of Tan et al. (2022).

Except for the intracellular components of DNA and proteins, the riboflavin-mediated PDI coupled with SBEW could also cause a high degree of lipid peroxide (LPO) in the cells of *Salmonella*. In Fig. 6C, all control samples did not show significant difference in the level of lipid peroxide, although a slight increase of LPO was observed. Notably, the photodynamic control (R + L + S-) just had a LPO level of 0.28 μM. As the irradiation dose increased to 15.6 J/cm^2, the LPO value was sharply increased to 1.05 μM under the action of PDI coupled with SBEW, which was ~4 times than that of the photodynamic control (R + L + S-). Lipid peroxidation can be described generally as a process under which oxidants such as free radicals attack lipids containing carbon-carbon double bond, especially polyunsaturated fatty acids (PUFAs) (Ayala et al., 2014). From the results of Fig. 4, the riboflavin-mediated PDI generated massive ROS in the presence of SBEW, and these free radicals attacked the PUFAs to induce a high level of LPO, and conversely, the high LPO caused serious damages to the structure and function of cell membranes and finally resulted in the death of cells.

Alkaline phosphatase (ALP) is a ubiquitous membrane-bound glycoprotein that catalyzes the hydrolysis of phosphate monoesters at basic pH values, and it is located between the cell wall and cell membrane, which is difficult to be determined in the supernatant of intact cells (Gao et al., 2014). As shown in Fig. 7A, all control samples presented almost the same ALP values (~0.13 mg/100 mL), and no significant difference was monitored. It was evident that the treatment of PDI coupled with SBEW obviously heightened the ALP values from 0.13 to 0.22 mg/100 mL, with the increase of irradiation dose from 6.24 to 15.6 J/cm^2. Meanwhile, the integrity of cell membranes was also evaluated by detecting the leakage of intracellular proteins (Shu et al., 2019). Likewise, all control samples displayed almost the same content of proteins (137 μg/mL) in the supernatant of intact cells (Fig. 7B), and these secretory proteins were highly derived from the normal metabolic activity of bacteria. With the increase of irradiation dose to 15.6 J/cm^2, the content of proteins in the supernatant was significantly increased to 231 μg/mL, and approximately 70% of the extra proteins were leaked to the outside of cells in comparison with the normal cells (137 μg/mL). Based on the above results, the PDI coupled with SBEW treatment greatly destroyed the cell membrane integrity of *Salmonella* to reduce its viability under the irradiation of blue LED.

3.3. Inactivation of the riboflavin-mediated PDI coupled with SBEW against Salmonella on tuna fillets

The application feasibility of the riboflavin-mediated PDI coupled with SBEW in inactivating *Salmonella* on the tuna fillets was investigated. In Fig. 8A, the tuna fillets samples were artificially contaminated with ~5.2 Log_{10} CFU/g of *Salmonella*. All control samples did not exhibit an obvious decrease of the cells after the corresponding treatment. However, the riboflavin-mediated PDI coupled with SBEW gradually decreased the colonies of *Salmonella* to 1.9 Log_{10} CFU/g ($P < 0.05$) with the increase of riboflavin concentration to 100 μM, and only 0.94 Log_{10} CFU/g could be detected on tuna fillets ($P < 0.05$) when the riboflavin concentration was increased to 120 μM, under the irradiation of 18.72 J/cm^2. Meanwhile, the effects of different irradiation doses on the inactivation of *Salmonella* on the tuna fillets were also explored (Fig. 8B). Overall speaking, the bactericidal potency of this novel PDI against *Salmonella* on the tuna fillets was irradiation dose-dependent when the irradiation dose was ≤18.72 J/cm^2, which meant that the increased irradiation dose enhanced the reduction of *Salmonella* on the tuna fillets during the PDI treatment. With the increase of irradiation (>18.72 J/cm^2), the PDI coupled with SBEW did not further cause significant reduction of *Salmonella* on the tuna fillets (Fig. 8B).

Huang et al. (2021) and Chen et al. (2021) showed that in comparison with planktonic cells in solution, a relatively higher curcumin (>100 μM) and irradiation dose (>9.36 J/cm^2) were needed to efficiently inactivate *Listeria monocytogenes* on salmon or *Vibrio parahaemolyticus* on cooked oysters by selecting the deionized water as the solvent to dissolve curcumin, and such facts proved that the natural photosensitizer-mediated PDI displayed difficulties in killing the bacteria on seafood. Although the phenomenon, the curcumin-mediated PDI still significantly ($P < 0.05$) retarded the increase in pH, the production of TVB-N, and suppressed the lipids oxidation of salmon and oysters, which was highly caused by the bacterial proliferation. Meanwhile, the PDI treatment also obviously inhibited the color changes of

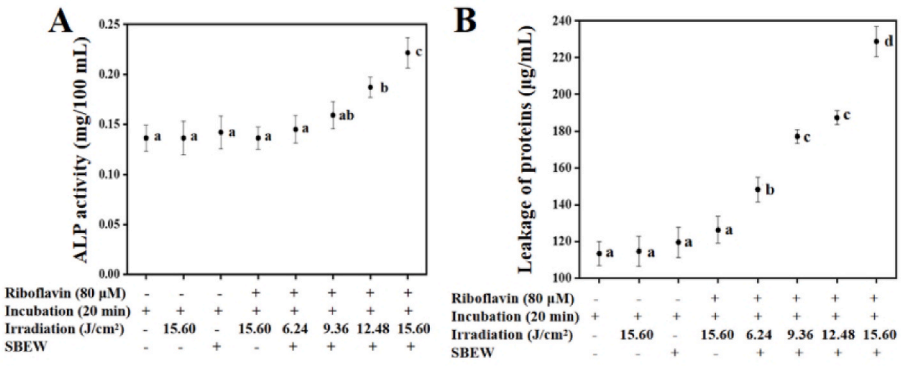

Fig. 7. Effects of the riboflavin-mediated PDI coupled with slightly basic electrolyzed water (SBEW) on the activity of alkaline phosphatase (A) and the leakage of proteins (B) in *Salmonella*.

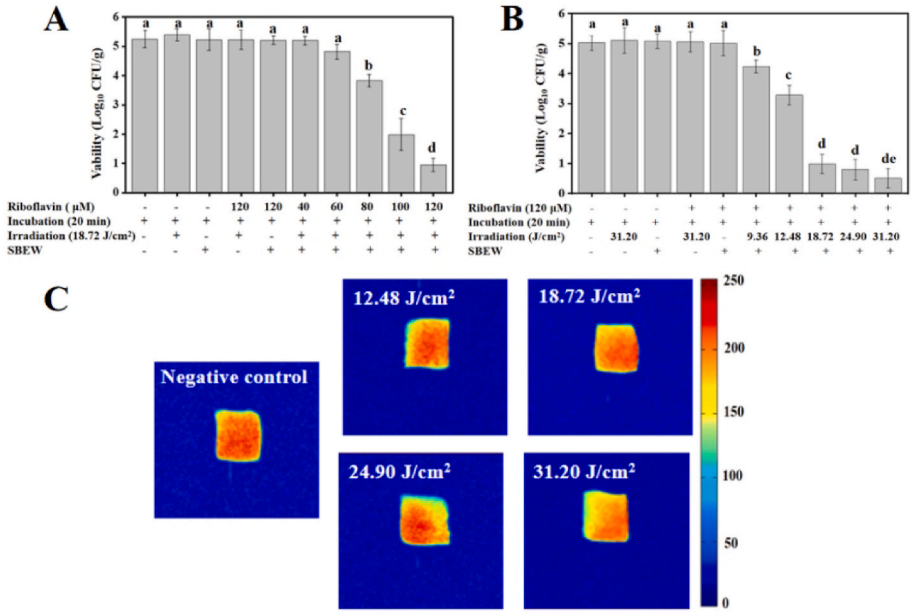

Fig. 8. Effects of the riboflavin-mediated PDI coupled with slightly basic electrolyzed water (SBEW) on the viability of *Salmonella* and water distribution in the fillets of tuna. (A) Riboflavin concentration; (B) Irradiation dosage; (C) Magnetic resonance imaging.

salmon in comparison with the control samples (Chen et al., 2021; Huang et al., 2021). Lan et al. (2021) also found that the common PDI could just kill ~1.0 Log_{10} CFU/g of *Salmonella* on the tuna fillets with the high riboflavin concentration of 150 μM and blue LED irradiation of 56.16 J/cm^2. Chen et al. (2021) concluded that such differences in the bactericidal potency of PDI should be highly attributed to the protective effects of the surface and substance composition of various foods, which provides crevices and fatty layers for the bacterial cells to hide and hence be shielded from the irradiation of light. In the present study, the riboflavin-mediated PDI coupled with SBEW could maximally kill ~4.0 Log_{10} CFU/g of *Salmonella* on the tuna fillets with the riboflavin concentration of 120 μM and blue LED irradiation of 18.72 J/cm^2 (Fig. 8B), which was significantly ($P < 0.05$) higher than those (93.6 J/cm^2) reported in the study of Lan et al. (2021).

Water is an important indicator of freshness for seafood, and hence the low-field nuclear magnetic resonance (LF-NMR) was applied to observe the effects of PDI treatment on the distribution of water molecules in the tuna fillets, with the purpose of reflecting their freshness changes (Chen et al., 2021). Generally, the color shift from red to blue represents the changes of high proton density to low one in the pseudo-color images (Chen et al., 2021; Huang et al., 2021). In Fig. 8C, the negative control samples presented a bright red color, indicating a high distribution of water molecules in the tuna fillets. After the irradiation of 12.48 and 18.72 J/cm^2, the PDI-treated samples still showed a red color, and an obvious shift of color was not observed, indicating that such irradiation dose of blue LED did not cause the loss of water in the tuna fillets. With the increase of irradiation dose to 24.90 and 31.20 J/cm^2, the treated samples displayed a reduced brightness of red color and a slightly increased blue color around the edge of tuna fillets, which suggested that the content of water decreased due to evaporation under irradiation (Ghosh et al., 2008). Considering the potent inactivation of *Salmonella* on the tuna fillets, this study proves that the riboflavin-mediated PDI coupled with SBEW treatment cannot produce greatly negative effects on the distribution of water molecules in tuna fillets with the appropriate irradiation dose of 18.72 J/cm^2, which is favorable for the preservation of the freshness of tuna fillets.

In addition, the effects of riboflavin-mediated PDI coupled with SBEW on the storage quality of tuna fillets were also investigated. In Fig. 9A, the initial cells of *Salmonella* on tuna fillets were ~5.4 Log CFU/g. The photodynamic control (R + L + S-) did not obviously decreased *Salmonella*, while the riboflavin-mediated PDI coupled with SBEW decreased *Salmonella* to ~0.70 Log CFU/g on tuna fillets, which meant that 4.7 Log CFU/g of *Salmonella* were inactivated. During the whole storage for 7 days at 10 °C, the viable bacteria in the novel PDI-treated samples were always lower ($P < 0.05$) than those in all control samples (R + L + S- and R-L-S-), proving that the riboflavin-mediated PDI coupled with SBEW was more effective in retarding the proliferation of *Salmonella* on tuna fillets during storage.

The electrical conductivity of the treated tuna fillets is presented in Fig. 9B. At day 0, the electrical conductivity of tuna fillets was ~104 μs/cm^2, and with the extension of storage, all tuna fillets displayed an increased electrical conductivity. However, the tuna fillets treated by the novel PDI showed a significantly ($P < 0.05$) lower electrical conductivity than all control samples (R + L + S- and R-L-S-). During the storage, the microbial action decomposed proteins, fats, and other substances into small biomolecules and ions, which contributed to the increase of electrical conductivity of tuna fillets (Fan et al., 2014). In this study, the PDI coupled with SBEW could effectively kill the bacteria and limited the microbial action, which decreased the electrical conductivity.

The pH changes of the treated tuna fillets are presented in Fig. 9C. The initial pH of tuna fillets reached ~7.6, and the pH of negative control (R-L-S-) decreased first and then increased during the whole storage. In general, the production of lactic acid and pyruvate by anaerobic glycolysis of glycogen decreased pH after biological death, and then the microorganism degraded the muscle protein to generate amines which increased pH. Similar results have been found in shrimp (Li et al., 2023) and salmon (Huang et al., 2021). Lipid oxidation causes deterioration in the freshness and nutrient values of fish products, and MDA is often used to determine the degree of lipid oxidation caused by microorganisms and endogenous enzymes (Lan et al., 2021; Wang et al., 2021). In Fig. 9D, all tuna fillets had an initial MDA value of ~3 nmol/g, and the values significantly increased with the extension of storage. However, the MDA (12.90 nmol/g) of tuna fillets treated by this novel PDI presented a low value compared to that (14.52 nmol/g) in the photodynamic control (R + L + S-) at the 7th day storage. All MDA values were significantly ($P < 0.05$) lower than that of negative control (24.73 nmol/g). These results suggested that the riboflavin-mediated PDI coupled with SBEW greatly decreased the lipid oxidation of tuna fillets.

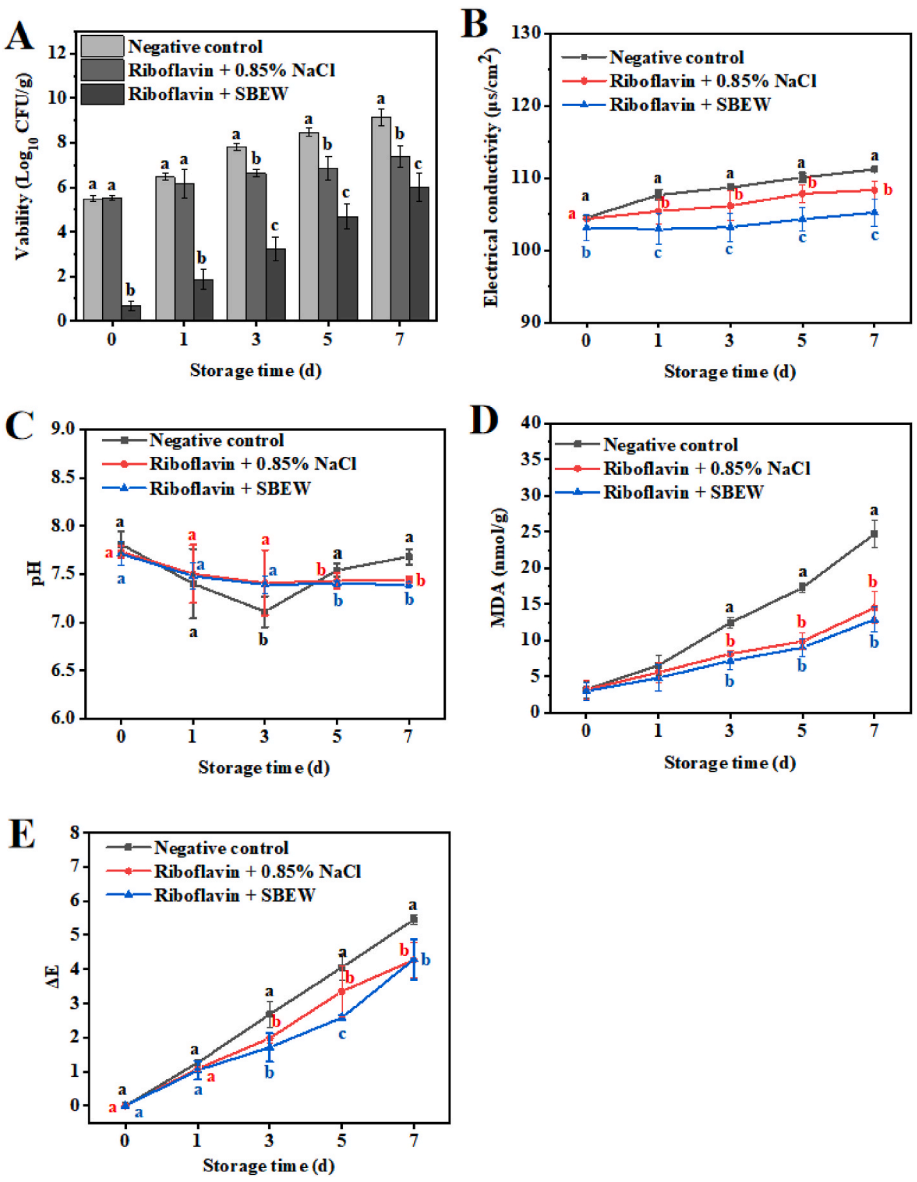

Fig. 9. Effects of the riboflavin-mediated PDI coupled with slightly basic electrolyzed water (SBEW) on the viability of *Salmonella* (A), electrical conductivity (B), pH (C), MDA (D), and ΔE (E) in tuna fillets during the storage for 7 days at 10 °C.

Color is an important sensory attribute of fillet products, which directly affects the consumer's acceptance. A large amount of myoglobin and hemoglobin in tuna fillets can be easily oxidized, which makes the fillets brown red. In Fig. 9E, the ΔE presented an increasing trend for all tuna fillets with the extension of storage (Shiekh & Benjakul, 2020). In detail, the negative control (R-L-S-) displayed an increase of ΔE from 0 to 5.45, which was significantly ($P < 0.05$) higher than all treated samples during the whole storage. The tuna fillets treated by the common PDI coupled with 0.85% NaCl showed an increase of ΔE from 0 to 4.3, but those treated by this novel PDI presented a much lower ΔE value, and especially after 5 days storage. Based on the above facts, the riboflavin-mediated PDI coupled with SBEW showed a stronger ability to inactivate the bacteria in tuna fillets compared to the common PDI coupled with 0.85% NaCl, and also presented a great potential in decelerating the bacterial proliferation, the changes of electrical conductivity, pH and color, and the lipid oxidation during the storage.

4. Conclusion

The SBEW was selected as the solvent to dissolve the photosensitizer of riboflavin, and its special physicochemical properties promoted the solubility of riboflavin, increased the production of ROS, especially the singlet oxygen ($^1O_2$) under the blue LED irradiation. Compared with the normal saline as the solvent, the SBEW enhanced the bactericidal ability of riboflavin-mediated PDI against *Salmonella* in solution. The action mechanisms showed that the riboflavin-mediated PDI coupled with SBEW destroyed the integrity of cell wall, induced the leakage of cellular contents, degraded the genomic DNA, and enhanced the lipid peroxidation in the cells of *Salmonella*. More importantly, this novel PDI could be applied to effectively kill *Salmonella* on tuna fillets, and retarded the bacterial proliferation, limited the changes of electrical conductivity, pH and color, and decreased the degree of lipid oxidation during the post-treatment storage of tuna fillets. Therefore, this study develops a new and effective non-thermal antibacterial technology to preserve the storage quality of seafood.

CRediT authorship contribution statement

Jing Jing Wang: Writing – review & editing, Supervision, Methodology, Funding acquisition, Conceptualization. **Tiantian He:**

Methodology, Investigation, Software, Writing-original draft. **Huihui Li:** Investigation, Software, Data curation. **Hao Dong:** Validation, Resources. **Yang Liu:** Validation. **Qiaohui Zeng:** Investigation, Resources. **Yong Zhao:** Writing – review & editing, Supervision, Funding acquisition, Conceptualization.

Declaration of competing interest

The authors declare that they have no known competing financial interests or personal relationships that could have appeared to influence the work reported in this paper.

Data availability

Data will be made available on request.

Acknowledgements

This work was supported by the National Natural Science Foundation of China (32102105); Program of Shanghai Academic Research Leader (21XD1401200); Guangdong Provincial Key Laboratory of Intelligent Food Manufacturing (2022B1212010015); Guangdong Basic and Applied Basic Research Foundation (2020A1515110960).

Appendix A. Supplementary data

Supplementary data to this article can be found online at https://doi.org/10.1016/j.foodcont.2024.110441.

References

Alves, E., Faustino, M. A., Neves, M. G., Cunha, A., Nadais, H., & Almeida, A. (2015). Potential applications of porphyrins in photodynamic inactivation beyond the medical scope. *Journal of Photochemistry and Photobiology C: Photochemistry Reviews, 22*, 34–57.

Ashoori, M., & Saedisomeolia, A. (2014). Riboflavin (vitamin B_2) and oxidative stress: A review. *British Journal of Nutrition, 111*(11), 1985–1991.

Ayala, A., Muñoz, M. F., & Argüelles, S. (2014). Lipid peroxidation: Production, metabolism, and signaling mechanisms of malondialdehyde and 4-hydroxy-2-nonenal. *Oxidative Medicine and Cellular Longevity*, 2014.

Beztsinna, N., Solé, M., Taib, N., & Bestel, I. (2016). Bioengineered riboflavin in nanotechnology. *Biomaterials, 80*, 121–133.

Chen, B. W., Huang, J. M., Li, H. H., Zeng, Q. H., Wang, J. J., Liu, H. Q., … Zhao, Y. (2020). Eradication of planktonic *Vibrio parahaemolyticus* and its sessile biofilm by curcumin-mediated photodynamic inactivation. *Food Control, 113*, Article 107181.

Chen, B. W., Huang, J. M., Liu, Y., Liu, H. Q., Zhao, Y., & Wang, J. J. (2021). Effects of the curcumin-mediated photodynamic inactivation on the quality of cooked oysters with *Vibrio parahaemolyticus* during storage at different temperature. *International Journal of Food Microbiology, 345*, Article 109152.

Chen, L., Zhao, Y., Wu, W. L., Zeng, Q. H., & Wang, J. J. (2023). New trends in the development of photodynamic inactivation against planktonic microorganisms and their biofilms in food system. *Comprehensive Reviews in Food Science and Food Safety*, 1–34.

Dolmans, D. E., Fukumura, D., & Jain, R. K. (2003). Photodynamic therapy for cancer. *Nature Reviews Cancer, 3*(5), 380–387.

Fan, H. B., Luo, Y. K., Yin, X. F., Bao, Y. L., & Feng, L. G. (2014). Biogenic amine and quality changes in lightly salt-and sugar-salted black carp (Mylopharyngodon piceus) fillets stored at 4°C. *Food Chemistry, 159*, 20–28.

Gao, A., Hang, R. Q., Huang, X. B., Zhao, L. Z., Zhang, X. Y., Wang, L., … Chu, P. K. (2014). The effects of titania nanotubes with embedded silver oxide nanoparticles on bacteria and osteoblasts. *Biomaterials, 35*(13), 4223–4235.

Ghosh, P. K., Jayas, D. S., Smith, E. A., Gruwel, M. L. H., White, N. D. G., & Zhilkin, P. A. (2008). Mathematical modelling of wheat kernel drying with input from moisture movement studies using magnetic resonance imaging (MRI), Part I: Model development and comparison with MRI observations. *Biosystems Engineering, 100*(3), 389–400.

Henry, M., & Chambron, J. (2013). Physico-chemical, biological and therapeutic characteristics of electrolyzed reduced alkaline water (ERAW). *Water, 5*(4), 2094–2115.

Hong, E. J., Choi, D. G., & Shim, M. S. (2016). Targeted and effective photodynamic therapy for cancer using functionalized nanomaterials. *Acta Pharmaceutica Sinica B, 6*(4), 297–307.

Hu, J. M., Lin, S. M., Tan, B. K., Hamzah, S. S., Lin, Y., Kong, Z., … Zeng, S. (2018). Photodynamic inactivation of *Burkholderia cepacia* by curcumin in combination with EDTA. *Food Research International, 111*, 265–271.

Huang, J. M., Chen, B. W., Li, H. H., Zeng, Q. H., Wang, J. J., Liu, H. Q., … Zhao, Y. (2020). Enhanced antibacterial and antibiofilm functions of the curcumin-mediated photodynamic inactivation against *Listeria monocytogenes*. *Food Control, 108*, Article 106886.

Huang, J. M., Chen, B. W., Zeng, Q. H., Liu, Y., Liu, H. H., Zhao, Y., & Wang, J. J. (2021). Application of the curcumin-mediated photodynamic inactivation for preserving the storage quality of salmon contaminated with *L. monocytogenes*. *Food Chemistry, 359*, Article 129974.

Lan, W. Q., Lang, A., Zhou, D. P., & Xie, J. (2021). Combined effects of ultrasound and slightly acidic electrolyzed water on quality of sea bass (Lateolabrax Japonicus) fillets during refrigerated storage. *Ultrasonics Sonochemistry, 81*, Article 105854.

LeBaron, T. W., Sharpe, R., & Ohno, K. (2022). Electrolyzed-reduced water: Review II: Safety concerns and effectiveness as a source of hydrogen water. *International Journal of Molecular Sciences, 23*(23), Article 14508.

Li, R. H., Jiang, Z. P., Yang, H. W., & Guan, Y. T. (2006). Effects of ions in natural water on the ^{17}O NMR chemical shift of water and their relationship to water cluster. *Journal of Molecular Liquids, 126*(1–3), 14–18.

Li, H. H., Tan, L. J., Chen, B. W., Huang, J. M., Zeng, Q. H., Liu, H. Q., … Wang, J. J. (2021). Antibacterial potency of riboflavin-mediated photodynamic inactivation against *Salmonella* and its influences on tuna fillets quality. *Lebensmittel-Wissenschaft und -Technologie, 146*, Article 111462.

Li, Y. F., Tan, L. J., Liu, F. Y., Li, M. Y., Zeng, S. Y., Gui, Y. L., … Wang, J. J. (2023). Effects of soluble Antarctic krill protein-curcumin complex combined with photodynamic inactivation on the storage quality of shrimp. *Food Chemistry, 403*, Article 134388.

Liu, J. J., Yu, S. Y., Han, B. Z., & Chen, J. Y. (2017). Effects of benzalkonium chloride and ethanol on dual-species biofilms of *Serratia liquefaciens S1* and *Shewanella putrefaciens S4*. *Food Control, 78*, 196–202.

Luksiene, Z., Buchovec, I., & Paskeviciute, E. (2009). Inactivation of food pathogen *Bacillus cereus* by photosensitization in *vitro* and on the surface of packaging material. *Journal of Applied Microbiology, 107*(6), 2037–2046.

Misba, L., Zaidi, S., & Khan, A. U. (2018). Efficacy of photodynamic therapy against *Streptococcus* mutans biofilm: Role of singlet oxygen. *Journal of Photochemistry and Photobiology B: Biology, 183*, 16–21.

Park, J. S., & Ha, J. W. (2020). Synergistic antimicrobial effect of X-ray and curcumin against *Listeria monocytogenes* on sliced cheese. *Food Control, 110*, Article 106986.

Rastogi, R. P., Singh, S. P., Häder, D. P., & Sinha, R. P. (2010). Detection of reactive oxygen species (ROS) by the oxidant-sensing probe 2′, 7′-dichlorodihydrofluorescein diacetate in the cyanobacterium Anabaena variabilis PCC 7937. *Biochemical and Biophysical Research Communications, 397*(3), 603–607.

Rubik, B. (2011). Studies and observations on the health effects of drinking electrolyzed-reduced alkaline water. *Water and Society, 153*, 321–327.

Sadraeian, M., Zhang, L., Aavani, F., Biazar, E., & Jin, D. (2022). Photodynamic viral inactivation assisted by photosensitizers. *Materials Today Physics*, Article 100882.

Shiekh, K. A., & Benjakul, S. (2020). Effect of pulsed electric field treatments on melanosis and quality changes of Pacific white shrimp during refrigerated storage. *Journal of Food Processing and Preservation, 44*(1), Article e14292.

Shirahata, S., Kabayama, S., Nakano, M., Miura, T., Kusumoto, K., Gotoh, M., … Katakura, Y. (1997). Electrolyzed–reduced water scavenges active oxygen species and protects DNA from oxidative damage. *Biochemical and Biophysical Research Communications, 234*(1), 269–274.

Shu, Q., Niu, Y., Zhao, W. J., & Chen, Q. H. (2019). Antibacterial activity and mannosylerythritol lipids against vegetative cells and spores of *Bacillus cereus*. *Food Control, 106*, Article 106711.

Tan, L. J., Li, H. H., Chen, B. W., Huang, J. M., Li, Y., Zheng, H. M., … Wang, J. J. (2021). Dual-species biofilms formation of *Vibrio parahaemolyticus* and *Shewanella putrefaciens* and their tolerance to photodynamic inactivation. *Food Control, 125*, Article 107983.

Tan, L. J., Zhao, Y., Li, Y. F., Peng, Z. Y., He, T. T., Liu, Y., … Wang, J. J. (2022). Potent eradication of mixed-species biofilms using photodynamic inactivation coupled with slightly alkaline electrolyzed water. *Lebensmittel-Wissenschaft und -Technologie, 155*, Article 112958.

Wang, S. J., Duan, H. L., Zhang, W., & Li, J. W. (2007). Analysis of bacterial foodborne disease outbreaks in China between 1994 and 2005. *FEMS Immunology and Medical Microbiology, 51*(1), 8–13.

Wang, J. J., Liu, G., Huang, Y. B., Zeng, Q. H., Hou, Y., Li, L., … Hu, S. Q. (2017). Dissecting the disulfide linkage of the N-terminal domain of HMW 1Dx5 and its contributions to dough functionality. *Journal of Agricultural and Food Chemistry, 65*(30), 6264–6273.

Wang, Z. M., Tu, J. C., Zhou, H., Lu, A., & Xu, B. C. (2021). A comprehensive insight into the effects of microbial spoilage, myoglobin autoxidation, lipid oxidation, and protein oxidation on the discoloration of rabbit meat during retail display. *Meat Science, 172*, Article 108359.

Wu, J., Mou, H. J., Xue, C. H., Leung, A. W., Xu, C. S., & Tang, Q. J. (2016). Photodynamic effect of curcumin on *Vibrio parahaemolyticus*. *Photodiagnosis and Photodynamic Therapy, 15*, 34–39.

Yan, Y., Ou, X. X., Zhang, H. P., & Shao, Y. (2013). Effects of nano-materials on ^{17}O NMR line-width of water clusters. *Journal of Molecular Structure, 1051*, 211–214.

Yan, Y. Y., Tan, L. J., Li, H. H., Chen, B. W., Huang, J. M., Zhao, Y., … Ou, J. (2021). Photodynamic inactivation of planktonic *Staphylococcus aureus* by sodium magnesium chlorophyllin and its effect on the storage quality of lettuce. *Photochemical and Photobiological Sciences, 20*(6), 761–771.

Yu, J. S., Zhang, F., Zhang, J., Han, Q. M., Song, L. L., & Meng, X. H. (2021). Effect of photodynamic treatments on quality and antioxidant properties of fresh-cut potatoes. *Food Chemistry, 362*, Article 130224.

Yue, M. N., Li, X. Y., Liu, D., & Hu, X. (2020). Serotypes, antibiotic resistance, and virulence genes of *Salmonella* in children with diarrhea. *Journal of Clinical Laboratory Analysis, 34*(12), Article e23525.

Zhang, L. N., Fu, Y., Xiong, Z. Y., Ma, Y. B., Wei, Y. H., Qu, X. Y., … Liao, M. (2018). Highly prevalent multidrug-resistant *Salmonella* from chicken and pork meat at retail markets in Guangdong, China. *Frontiers in Microbiology, 9*, 2104.

Zhang, L. T., Huang, X. H., Miao, S., Zeng, S. X., Zhang, Y., & Zheng, B. D. (2016). Influence of ultrasound on the rehydration of dried sea cucumber (Stichopus japonicus). *Journal of Food Engineering, 178*, 203–211.

Zhao, X. L., & Drlica, K. (2014). Reactive oxygen species and the bacterial response to lethal stress. *Current Opinion in Microbiology, 21*, 1–6.